

DOI: 10.1002/cmdc.201402362

# Drug Delivery to the Malaria Parasite Using an Arterolane-Like Scaffold

Shaun D. Fontaine,<sup>[a]</sup> Benjamin Spangler,<sup>[a]</sup> Jiri Gut,<sup>[b]</sup> Erica M. W. Lauterwasser,<sup>[a]</sup> Philip J. Rosenthal,<sup>[b]</sup> and Adam R. Renslo<sup>\*[a]</sup>

Antimalarial agents artemisinin and arterolane act via initial reduction of a peroxide bond in a process likely mediated by ferrous iron sources in the parasite. Here, we report the synthesis and antiplasmodial activity of arterolane-like 1,2,4-trioxolanes specifically designed to release a tethered drug species within the malaria parasite. Compared with our earlier drug delivery scaffolds, these new arterolane-inspired systems are of significantly decreased molecular weight and possess superior metabolic stability. We describe an efficient, concise and scalable synthesis of the new systems, and demonstrate the use of the aminonucleoside antibiotic puromycin as a chemo/biomarker to validate successful drug release in live *Plasmodium falciparum* parasites. Together, the improved drug-like properties, more efficient synthesis, and proof of concept using puromycin, suggests these new molecules as improved vehicles for targeted drug delivery to the malaria parasite.

Peroxicidal antimalarials, such as the artemisinins, trioxolanes (e.g., OZ439<sup>[1]</sup> and arterolane (1)<sup>[2,3]</sup>), and tetraoxanes,<sup>[4]</sup> exert their therapeutic effects via initial reduction of a hindered peroxide bond. While the point is still debated, it seems probable that this reduction is mediated by ferrous iron heme liberated during intraparasitic proteolysis of haemoglobin.<sup>[5–11]</sup> It appears then that these agents lack a “target” in the traditional sense and instead exploit an aberrant chemical environment produced through host–parasite interaction. Our group and others have shown that this reducing environment in the parasite can be exploited for parasite-selective drug delivery from suitably engineered endoperoxides,<sup>[12]</sup> trioxolanes,<sup>[13–15]</sup> or tetraoxanes.<sup>[16,17]</sup> Unlike “hybrid antimalarials”,<sup>[18,19]</sup> these drug delivery systems release their payload in an untethered form, free from any linker. Accordingly, this approach can be used to deliver existing antimalarial drugs with improved selectivity and decreased off-target toxicity.

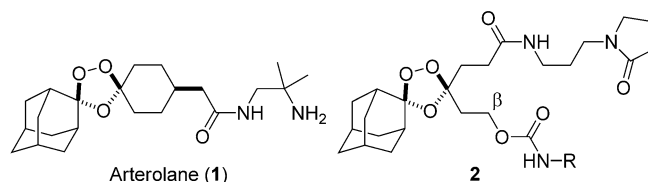


**Figure 1.** Structures of the antimalarial agent arterolane (1) and trioxolane conjugate 2, which confers parasite-selective delivery of a tethered dipeptidyl peptidase-1 (DPAP1) inhibitor (ML4118S or NH<sub>2</sub>-R in 2).

In our earlier studies, we employed trioxolane conjugate 2 (Figure 1) to establish the concept of trioxolane-mediated, ferrous-iron-dependent drug delivery.<sup>[13,15]</sup> The potent antimalarial ML4118S,<sup>[20]</sup> an inhibitor of the parasite cysteine protease dipeptidyl peptidase-1 (DPAP1), was employed as the drug species to be delivered from 2. Using activity-based probes, we established that conjugate 2 efficiently releases ML4118S in live *Plasmodium falciparum* parasites with a half-life ( $t_{1/2}$ ) estimated at 1.5 hours.<sup>[13]</sup> In the *P. berghei* in vivo model, we observed more sustained DPAP1 inhibition in mice receiving 2 than in mice administered ML4118S directly, and also saw greatly decreased off-target effects in 2-treated mice.<sup>[15]</sup> The use of non-peroxidic control compounds in this study established that the beneficial effects realized with 2 were indeed a result of trioxolane-mediated, parasite-selective drug delivery.

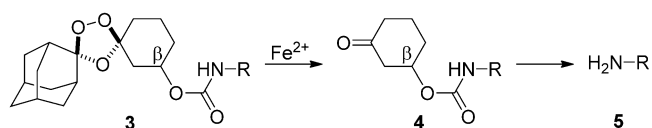
Although first-generation molecules like 2 proved invaluable to establish the concept, their high molecular weight and large number of rotatable bonds predicts less than optimal drug-like properties. Herein, we describe a new drug delivery scaffold (3) with greatly decreased molecular weight and generally superior drug-like properties. We also describe the use of the aminonucleoside antibiotic puromycin as a chemical–biological probe to validate drug delivery from 3 in live *P. falciparum* parasites.

As in our earlier systems, drug delivery from trioxolane 3 is achieved by the coupling of two reaction processes. First, reduction of the peroxide bond in 3 and trioxolane fragmentation leads to ketone 4 in which drug is tethered at the  $\beta$  position. Release of free drug (5) from 4 then occurs by spontaneous retro-Michael reaction and decarboxylation (Scheme 1). Significantly, the carbamate linkage in 3 is stable, but becomes labile upon unmasking of the ketone function in intermediate 4. Compared with 2, second-generation conjugates 3 are  $\approx$  150 Da lower in molecular weight and structurally more closely related to successful drug candidates, such as arterolane and OZ439. We therefore anticipated that conjugates 3 should possess drug-like properties superior to 2.

[a] Dr. S. D. Fontaine, B. Spangler, Dr. E. M. W. Lauterwasser, Prof. Dr. A. R. Renslo  
Department of Pharmaceutical Chemistry  
University of California, San Francisco  
1700 4th Street, San Francisco, CA 94158 (USA)  
E-mail: adam.renslo@ucsf.edu

[b] Dr. J. Gut, Prof. Dr. P. J. Rosenthal  
Department of Medicine, University of California, San Francisco  
1001 Potrero Ave, San Francisco, CA (USA)

Supporting information for this article is available on the WWW under <http://dx.doi.org/10.1002/cmdc.201402362>.

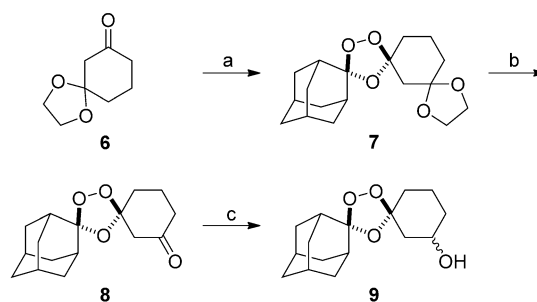


**Scheme 1.**  $\text{Fe}^{\text{II}}$ -mediated reduction of trioxolane **3** leads to retro-Michael intermediate **4**, which subsequently releases free drug **5** after  $\beta$ -elimination and decarboxylation.

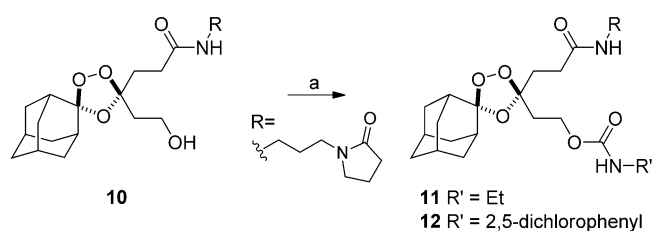
While 1,2,4-trioxolanes have been widely studied as antimalarial agents, analogues substituted at the 3-position of the cyclohexane ring (as in **3**) have been scarcely explored.<sup>[21,22]</sup> We therefore sought to develop a general synthetic approach to prepare such analogues. Gratifyingly, we found that partially protected diketone **6** participates in Griesbaum co-ozonolysis with *O*-methyl 2-adamantanone oxime to afford the desired trioxolane **7** in nearly quantitative yields (Scheme 2). Notably, the use of two or more equivalents of oxime in this reaction was essential to achieve high chemical yields. Deprotection of ketal **7** with ferric chloride hexahydrate in acetone/dichloromethane proceeded smoothly to afford ketone **8** in excellent yield. Using a modification of the conditions reported previously<sup>[23]</sup> for reductions of 4''-keto trioxolanes, we successfully reduced 3''-keto trioxolane **8** to the desired alcohol intermediate (**9**) in 67% yield. This reduction proceeded with little diastereofacial selectivity, affording **9** as a roughly equal mixture of *cis* and *trans* diastereoisomers (both racemic). The synthesis of **9** reported here (3 steps,  $\approx 63\%$  overall yield) compares favorably with our previous synthesis<sup>[13]</sup> of the analogous first-generation alcohol **10** (3 steps, 12% overall yield) used to prepare **2**. Although we have recently developed a diastereoselective synthesis of *trans*-**9** (to be described elsewhere), all compounds reported herein were prepared from the diastereomeric mixture of *cis* and *trans*-**9**.

To compare the first- and second-generation trioxolane scaffolds, we prepared congenic conjugates of alcohols **9** and **10** with ethylamine and 2,5-dichloroaniline. The ethyl carbamates were prepared to evaluate intrinsic antimalarial potency and in vitro ADME properties, while conjugates of 2,5-dichloroaniline were employed to study in vitro drug release rates (the aniline moiety affording a chromophore for spectroscopic detection). For the first-generation analogues, reaction of alcohol **10** with ethyl or 2,5-dichlorophenyl isocyanate afforded the desired carbamate **11** or **12**, respectively (Scheme 3). Second-generation comparators **13** and **14** were prepared from alcohol **9** under similar conditions and in comparable chemical yields (Scheme 4).

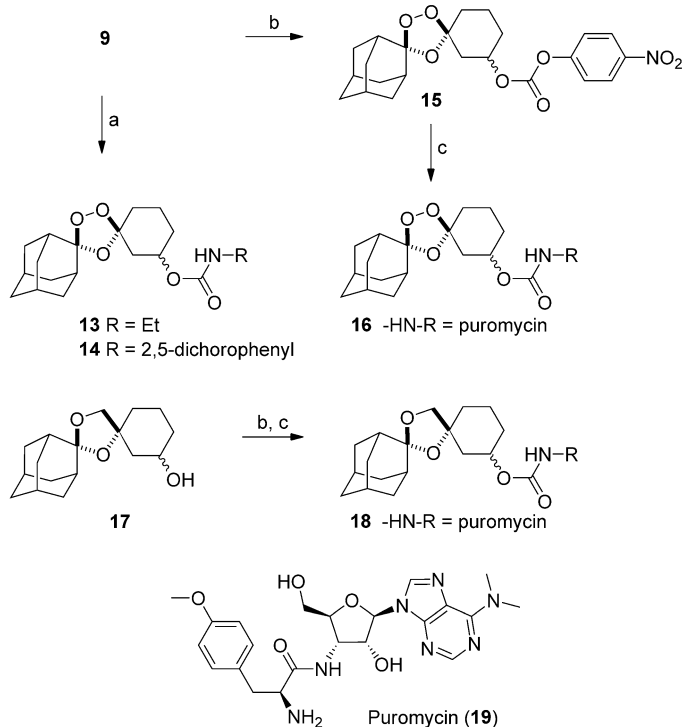
We compared the in vitro antiplasmodial activities and in vitro ADME properties of first-generation conjugates **11** and **12** with their second-generation congeners **13** and **14** (Table 1). All four compounds exhibited low nanomolar effects on the growth of cultured W2 *P. falciparum* parasites as determined using a flow-cytometry-based growth inhibition assay.<sup>[24]</sup>



**Scheme 2.** Reagents and conditions: a) 2.4 equiv *O*-methyl 2-adamantanone oxime,  $\text{CCl}_4$ ,  $\text{O}_3$ , 2.5 h,  $0^\circ\text{C}$ , 97%; b) 3 equiv  $\text{FeCl}_3 \cdot 6\text{H}_2\text{O}$ , acetone/ $\text{CH}_2\text{Cl}_2$  (5:1),  $0^\circ\text{C} \rightarrow \text{RT}$ , 1.5 h, 96%; c)  $\text{NaBH}_4$ , EtOH/THF (2:1),  $-78 \rightarrow 0^\circ\text{C}$ , 5 h, 67%.



**Scheme 3.** Reagents and conditions: a)  $\text{R}'\text{NCO}$ , pyridine, toluene,  $50^\circ\text{C}$ , 42 h, 71% (**11**), 63% (**12**).



**Scheme 4.** Reagents and conditions: a)  $\text{R}'\text{NCO}$ , pyridine, toluene,  $50^\circ\text{C}$ , 18–72 h, 74% (**13**), 55–79% (**14**); b)  $p\text{-NO}_2\text{C}_6\text{H}_4\text{OC(O)Cl}$ ,  $i\text{Pr}_2\text{NEt}$ , DMAP,  $\text{CH}_2\text{Cl}_2$ , 25 min,  $0^\circ\text{C} \rightarrow \text{RT}$ , 94% (**15**); c) **19**,  $i\text{Pr}_2\text{NEt}$ , DMAP, DMF, RT, 44 h, 61% (**16**); 52% over two steps (**18**).

Compd	$EC_{50}$ [nM] <sup>[a]</sup>	95% CI <sup>[b]</sup>	Rat CL <sup>[c]</sup>	In vitro drug release $t_{1/2}$	
				H <sub>2</sub> O/CH <sub>3</sub> CN <sup>[d]</sup>	DMEM/FBS <sup>[e]</sup>
ART <sup>[f]</sup>	7.1	6.1–8.4	–	–	–
<b>1</b>	4.8	2.7–8.4	59	–	–
<b>11</b>	16	11–24	694	–	–
<b>12</b>	0.39	0.32–0.46	–	5.3 h	–
<b>13</b>	12	11–14	155	–	–
<b>14</b>	13	11–15	–	170 h	9 min
<b>16</b>	10	9.1–12	–	–	–
<b>18</b>	> 1000	n.a.	–	–	–
<b>19</b>	42	32–56	–	–	–

[a] Potency against W2 *Plasmodium falciparum* parasites in cell culture; values are the average of three determinations; [b] 95% confidence interval for the  $EC_{50}$  values; [c] rat liver microsome stability, expressed as clearance (CL) in units of  $\mu\text{L min}^{-1} \text{mg}^{-1}$ ; [d] 100 equiv FeBr<sub>2</sub>, 0.3 mM in H<sub>2</sub>O/CH<sub>3</sub>CN (1:1); [e] 100 equiv FeBr<sub>2</sub>, 0.3 mM in high-glucose Dulbecco's modified eagle medium (DMEM) and 10% fetal bovine serum (FBS). [f] Artemisinin (ART).

Second-generation analogues **13** and **14** thus behave as typical trioxolane antimalarials and are presumably reduced in the parasite via the canonical iron(II)-mediated process. First- and second-generation ethyl carbamates **11** and **13** were evaluated for stability in the presence of cultured liver microsomes from human, rat, and mouse. In all cases, analogue **13** exhibited significantly improved metabolic stability as compared with first-generation conjugate **11**. The aqueous solubility of **11** and **13** was superior to **1**, while stability of the compounds in human and mouse plasma was comparable to **1** (Table S1 in the Supporting Information). With favorable ADME properties and significantly ( $\approx 150$  Da) lower molecular weight, second-generation trioxolane conjugates derived from **9** should have superior prospects for oral bioavailability and generally improved drug-like properties.

Next, we employed aryl carbamates **12** and **14** to study trioxolane fragmentation and drug release in vitro. Using liquid chromatography–mass spectrometry (LC/MS) instrumentation with evaporative light-scattering and mass detection, we were able to follow the iron(II)-mediated breakdown of parent compounds **12** and **14** to produce the corresponding retro-Michael intermediates and finally, liberated 2,5-dichloroaniline (a surrogate for released drug). Intrinsic reactivity with ferrous iron was evaluated using the in vitro conditions first recommended by Charman.<sup>[25]</sup> Hence, **12** and **14** were subjected to reaction with a 100-fold molar excess of iron(II) bromide in water/acetonitrile (1:1) at 37 °C. Both **12** and **14** were reduced rapidly under these conditions, with second-generation analogue **14** exhibiting a longer half-life of  $\approx 16$  min, as compared with  $\approx 2$  min for **12** (Table 1).

While ferrous-iron-promoted reduction of **12** and **14** was rapid in acetonitrile/water, we found that subsequent  $\beta$ -elimination and release of 2,5-dichloroaniline was very slow (hours to days) in this organic/aqueous solvent mixture (Table 1). These sluggish rates of  $\beta$ -elimination were not altogether reconcilable with our earlier findings that drug release from **2** occurs on therapeutically relevant time scales ( $t_{1/2} \approx 1.5$  h),

both in cultured parasites and in animal models.<sup>[13,15]</sup> We therefore sought to identify more biologically relevant reaction media for in vitro studies of drug release from these systems. Interestingly, we found that reaction with iron(II) bromide in a common cell culture media comprising high-glucose Dulbecco's modified eagle medium (DMEM) and 10% fetal bovine serum (FBS) resulted in drug release rates more in accord with our previous in vivo and cell culture results. Thus, in DMEM/FBS, release of 2,5-dichloroaniline from **14** was complete within 60–90 min, with a half-life of  $\approx 9$  min (Table 1 and Figure 2). Trioxolane activation occurs too rapidly in this media to determine a half-life for the iron-promoted reduction step. While release rates might be underestimated in water/acetonitrile and overestimated in DMEM/FBS, we found under both conditions that the retro-Michael reaction is the rate-determining step in drug release.

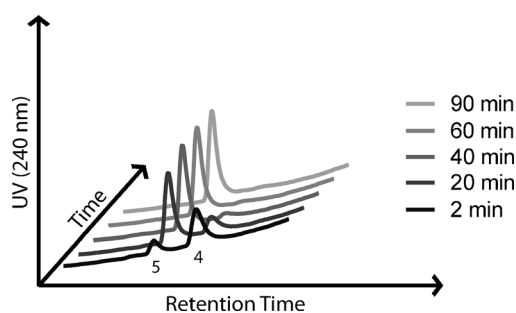


**Figure 2.** Chromatograms showing generation of the retro-Michael intermediate (**4**) and subsequent release of 2,5-dichloroaniline (**5**) following reaction of **14** with iron(II) bromide in Dulbecco's modified eagle medium (DMEM) and 10% fetal bovine serum (FBS).

In our previous studies with **2**, we employed activity-based probes to demonstrate the efficient release of tethered ML4118S in parasites. Here, we report another approach to study drug release in parasites by using trioxolane conjugates of the aminonucleoside antibiotic puromycin (**19**; Scheme 4). Puromycin acts by mimicking the 3' end of tyrosine tRNA and becomes incorporated into growing polypeptides at the ribosome, eventually causing premature chain termination and the release of puromycin-containing peptides. Notably, these puromycin-polypeptides can be detected with  $\alpha$ -puromycin antibodies. Previously, this activity of puromycin was used to validate protease-activated prodrugs in mammalian cancer cell lines and xenograft models.<sup>[26]</sup> Puromycin is known to be toxic to *P. falciparum* in vitro, and the gene for puromycin *N*-acetyltransferase has been used as a selectable marker for manipulating the parasite genetically.<sup>[27]</sup> Thus, we became intrigued by the notion of using trioxolane–puromycin conjugates to study drug release in live *P. falciparum* parasites.

The requisite trioxolane–puromycin conjugate (**16**) was prepared in two steps and 59% overall yield from alcohol **9** (Scheme 4). The nonperoxidic puromycin conjugate (**18**) was prepared from alcohol **17** by an analogous procedure and serves as an important control (Scheme 4; see also the Sup-

porting Information). The  $\alpha$ -amine of puromycin is carbamoylated in **16** and **18**, and so the intact conjugates should be incapable of incorporation into parasite polypeptides. Exposure to ferrous iron in the parasite, however, is expected to release free puromycin from **16** (but not from **18**). Thus, the detection of puromycin incorporation in parasites treated with **16** (but not in those treated with **18**) would provide strong evidence for the trioxolane-mediated release of puromycin from **16**. As detailed below, this is precisely what we observed with conjugates **16** and **18**.

First, we evaluated the antiparasitic activity of puromycin itself (**19**) as well as its two conjugates **16** and **18**. As expected, puromycin and its trioxolane conjugate **16** exhibited low nanomolar activity against W2 parasites, whereas nonperoxidic conjugate **18** was  $\approx 100$ -fold less potent (Table 1). This result confirms that the toxicity of puromycin is largely ablated when conjugated at the  $\alpha$ -amine, as expected. Next, we employed puromycin (**19**), trioxolane–puromycin conjugate **16**, and nonperoxidic control **18** to study peroxide-dependent drug release in live *P. falciparum* parasites. Synchronized trophozoite stage parasites, the erythrocytic stage when protein synthesis is most robust, were incubated with equimolar concentrations (400 nM) of compound **19**, **16**, or **18** for up to 12 hours. Parasites were periodically released from erythrocytes by saponin lysis, and the isolated parasites were analyzed for total puromycin incorporation in parasite proteins using a “dot blot” analysis with  $\alpha$ -puromycin antibody (Figure S1 in the Supporting Information). Protein samples run on a sodium dodecyl sulfate–polyacrylamide gel electrophoresis (SDS–PAGE) gel and analyzed by Western blotting with  $\alpha$ -puromycin antibody confirmed that puromycin is incorporated broadly into the parasite proteome (Figure S2 in the Supporting Information).

The results of the puromycin studies were unambiguous and fully consistent with peroxide-dependent release of puromycin from **16**. Thus, parasites treated with either puromycin (**19**) or its trioxolane conjugate (**16**) showed a time-dependent increase in puromycin incorporation in parasite protein (Figure 3; see also Figure S1 in the Supporting Information). In contrast, parasites treated with dioxolane–puromycin conjugate **18** showed negligible puromycin incorporation over the course of the experiment. This finding both confirms the peroxide-dependence of puromycin release from **16** and also demonstrates that puromycin action and toxicity is largely ablated while in conjugated forms (as revealed also by the  $\approx 100$ -fold higher  $EC_{50}$  value for **18** vs **19**). The ability to block the activity/toxicity of a drug species prior to release in the parasite is a key advantage of trioxolane-mediated drug delivery and distinguishes this approach from hybrid antimalarials, which must necessarily remain active/toxic in their conjugated forms.

Also of note from these studies was the fact that puromycin incorporation appeared to be greater in parasites treated directly with puromycin (**19**) than in those treated with **16**. This difference appears to be a consequence of more rapid puromycin incorporation during the first hour in **19**-treated parasites (Figure 3). After this initial burst, rates of incorporation are similar (nearly equivalent slopes) between parasites treated with **19** and those treated with **16**. The difference in the early

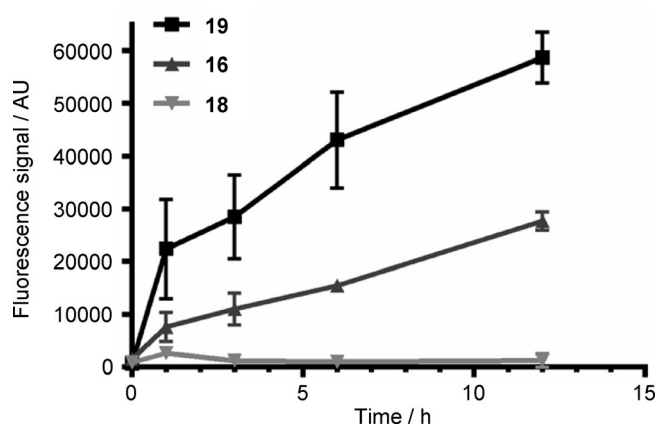


**Figure 3.** Quantification of puromycin incorporation in proteins of *Plasmodium falciparum* parasites treated with **19**, **16**, or **18**. Negligible puromycin incorporation was observed for dioxolane conjugate **18**, indicating that puromycin release from **16** is peroxide-dependent.

stages of treatment might reflect a lag in puromycin release from **16**, which is not unexpected given the results of our in vitro drug release studies, where complete release of free drug required 60–90 min (Figure 2). Alternatively, the difference might simply reflect the toxic effects of a trioxolane-based insult that is conferred to parasites by **16** but not **19**. Thus, the application of trioxolane **16** in excess of its  $EC_{50}$  value might reasonably be expected to affect rates of parasite growth and protein synthesis, leading to slower puromycin incorporation initially. Whatever the case, the dot blot studies with **19**, **16**, and **18** combined with the in vitro drug release studies described herein serve to validate **3** as a competent scaffold for drug delivery to *P. falciparum* parasites.

In conclusion, we have described an improved chemical scaffold for trioxolane-mediated drug delivery. The new molecules **3** are of significantly lower molecular weight, and exhibit superior drug-like properties when compared with our earlier systems. An efficient, concise and scalable synthesis of key synthetic intermediate **9** is described and should facilitate additional studies of these molecules in various applications. Finally, we have demonstrated the utility of the aminonucleoside puromycin as a chemical–biological marker to study drug release in *P. falciparum*. We anticipate that the use of puromycin as a drug surrogate will enable future studies of trioxolane-mediated drug delivery in malaria and other disease models.

## Acknowledgements

ARR acknowledges the support of the US National Institutes of Health (NIH) (R21AI0944233 and R01AI105106) and the Bill and Melinda Gates Foundation (USA). The authors thank Prof. Matthew Bogyo (Stanford University, USA) for helpful discussions and suggestions.

**Keywords:** antimalarial agents • drug delivery • *Plasmodium falciparum* • puromycin • targeted prodrugs • trioxolanes

- [1] S. A. Charman, S. Arbe-Barnes, I. C. Bathurst, R. Brun, M. Campbell, W. N. Charman, F. C. K. Chiu, J. Chollet, J. C. Craft, D. J. Creek, et al., *Proc. Natl. Acad. Sci. USA* **2011**, *108*, 4400–4405.
- [2] J. L. Vennerstrom, S. Arbe-Barnes, R. Brun, S. A. Charman, F. C. K. Chiu, J. Chollet, Y. Dong, A. Dorn, D. Hunziker, H. Matile, et al., *Nature* **2004**, *430*, 900–904.
- [3] Y. Dong, S. Wittlin, K. Sriraghavan, J. Chollet, S. A. Charman, W. N. Charman, C. Scheurer, H. Urwyler, J. Santo Tomas, C. Snyder, et al., *J. Med. Chem.* **2010**, *53*, 481–491.
- [4] F. Marti, J. Chadwick, R. K. Amewu, H. Burrell-Saward, A. Srivastava, S. a. Ward, R. Sharma, N. Berry, P. M. O'Neill, *MedChemComm* **2011**, *2*, 661.
- [5] P. M. O'Neill, G. H. Posner, *J. Med. Chem.* **2004**, *47*, 2945–2964.
- [6] Y. Tang, Y. Dong, X. Wang, K. Sriraghavan, J. K. Wood, J. L. Vennerstrom, *J. Org. Chem.* **2005**, *70*, 5103–5110.
- [7] R. K. Haynes, W. C. Chan, C.-M. Lung, A.-C. Uhlemann, U. Eckstein, D. Tar-amelli, S. Parapini, D. Monti, S. Krishna, *ChemMedChem* **2007**, *2*, 1480–1497.
- [8] D. J. Creek, W. N. Charman, F. C. K. Chiu, R. J. Prankerd, Y. Dong, J. L. Vennerstrom, S. A. Charman, *Antimicrob. Agents Chemother.* **2008**, *52*, 1291–1296.
- [9] P. M. O'Neill, V. E. Barton, S. A. Ward, *Molecules* **2010**, *15*, 1705–1721.
- [10] C. L. Hartwig, E. M. W. Lauterwasser, S. S. Mahajan, J. M. Hoke, R. A. Cooper, A. R. Renslo, *J. Med. Chem.* **2011**, *54*, 8207–8213.
- [11] R. K. Haynes, K.-W. Cheu, H.-W. Chan, H.-N. Wong, K.-Y. Li, M. M.-K. Tang, M.-J. Chen, Z.-F. Guo, Z.-H. Guo, K. Sinniah, et al., *ChemMedChem* **2012**, *7*, 2204–2226.
- [12] P. M. O'Neill, P. A. Stocks, M. D. Pugh, N. C. Araujo, E. E. Korshin, J. F. Bickley, S. A. Ward, P. G. Bray, E. Pasini, J. Davies, et al., *Angew. Chem. Int. Ed.* **2004**, *43*, 4193–4197; *Angew. Chem.* **2004**, *116*, 4289–4293.
- [13] S. S. Mahajan, E. Deu, E. M. W. Lauterwasser, M. J. Leyva, J. A. Ellman, M. Bogyo, A. R. Renslo, *ChemMedChem* **2011**, *6*, 415–419.
- [14] S. S. Mahajan, J. Gut, P. J. Rosenthal, A. R. Renslo, *Future Med. Chem.* **2012**, *4*, 2241–2249.
- [15] E. Deu, I. Chen, E. M. W. Lauterwasser, J. Valderramos, H. Li, L. Edgington, A. R. Renslo, M. Bogyo, *Proc. Natl. Acad. Sci. USA* **2013**, *110*, 18244–18249.
- [16] R. Oliveira, A. S. Newton, R. C. Guedes, D. Miranda, R. K. Amewu, A. Srivastava, J. Gut, P. J. Rosenthal, P. M. O'Neill, S. A. Ward, et al., *ChemMedChem* **2013**, *8*, 1528–1536.
- [17] R. Oliveira, R. C. Guedes, P. Meireles, I. S. Albuquerque, L. M. Gonçalves, E. Pires, M. R. Bronze, J. Gut, P. J. Rosenthal, M. Prudêncio, et al., *J. Med. Chem.* **2014**, *57*, 4916–4923.
- [18] B. Meunier, *Acc. Chem. Res.* **2008**, *41*, 69–77.
- [19] T.-S. Feng, E. M. Guantai, M. Nell, C. E. J. van Rensburg, K. Ncokazi, T. J. Egan, H. C. Hoppe, K. Chibale, *Biochem. Pharmacol.* **2011**, *82*, 236–247.
- [20] E. Deu, M. J. Leyva, V. E. Albrow, M. J. Rice, J. A. Ellman, M. Bogyo, *Chem. Biol.* **2010**, *17*, 808–819.
- [21] Y. Dong, J. Chollet, H. Matile, S. A. Charman, F. C. K. Chiu, W. N. Charman, B. Scoreaux, H. Urwyler, J. Santo Tomas, C. Scheurer, et al., *J. Med. Chem.* **2005**, *48*, 4953–4961.
- [22] Q. Zhao, M. Vargas, Y. Dong, L. Zhou, X. Wang, K. Sriraghavan, J. Keiser, J. L. Vennerstrom, *J. Med. Chem.* **2010**, *53*, 4223–4233.
- [23] Y. Tang, Y. Dong, J. M. Karle, C. A. DiTusa, J. L. Vennerstrom, *J. Org. Chem.* **2004**, *69*, 6470–6473.
- [24] P. S. Sijwali, K. Kato, K. B. Seydel, J. Gut, J. Lehman, M. Klemba, D. E. Goldberg, L. H. Miller, P. J. Rosenthal, *Proc. Natl. Acad. Sci. USA* **2004**, *101*, 8721–8726.
- [25] D. Creek, W. Charman, F. C. K. Chiu, R. J. Prankerd, K. J. Mccullough, Y. Dong, J. L. Vennerstrom, S. A. Charman, *J. Pharm. Sci.* **2007**, *96*, 2945–2956.
- [26] N. Ueki, S. Lee, N. S. Sampson, M. J. Hayman, *Nat. Commun.* **2013**, *4*, 2735.
- [27] T. F. de Koning-Ward, A. P. Waters, B. S. Crabb, *Mol. Biochem. Parasitol.* **2001**, *117*, 155–160.

Received: August 23, 2014

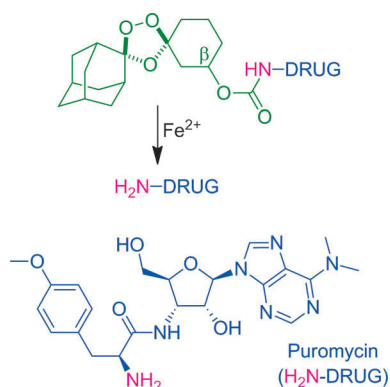
Published online on ■ ■ ■, 0000

## COMMUNICATIONS

S. D. Fontaine, B. Spangler, J. Gut,  
E. M. W. Lauterwasser, P. J. Rosenthal,  
A. R. Renslo\*



### Drug Delivery to the Malaria Parasite Using an Arterolane-Like Scaffold



**Let it go!** Targeted drug delivery to the malaria parasite is demonstrated with next-generation 1,2,4-trioxolanes closely related to antimalarial agents arterolane and OZ439. The new systems are prepared by an improved synthetic route and exhibit superior drug-like properties compared with their progenitors. Efficient release of a small-molecule payload is demonstrated with the aminonucleoside puromycin, which becomes incorporated into the *Plasmodium falciparum* proteome when released from a competent trioxolane conjugate.